2-D Localization and Identification Based on SAW ID-Tags at 2.5 GHz

Thomas F. Bechteler and Hüsnü Yenigün

***Abstract*—An identification and localization system based on surface acoustic wave (SAW) radio sensors is presented in this paper. This system is able to identify and localize objects within a two-dimensional area. Identification is done with a fixed coded passive SAW identification-tag. Localization is done with three receiving antennas and with a following analysis of time delay between the sent interrogation signal and the received signals. For practical tests, a special interrogator has been established, as well as the receiving and demodulation unit. The whole system is controlled by a computer.**

***Index Terms*—Identification, localization, RF identification-tag (ID-tag), surface acoustic wave (SAW).**

I. Introduction

IN RECENT years, the investigation of surface acoustic wave (SAW) devices shows a variety of applications. SAW devices are used as sensors [1]–[3], where special manufactured SAW chips can, for example, detect gases and measure velocity or pressure. They are also used in wireless identification systems [4], [5], where so-called SAW identification-tags (ID-tags) are used to identify objects. Inter alia, the identification with means of correlation, has been investigated [6], as well as the multiple access problem [7], [8], all SAW devices with the same distance to the transceiver unit. An interrogation unit for SAW radio transponder systems was presented in [5]. In what follows, a new application of SAW ID-tags is presented. The new aspect in this study is to combine the identification with the localization of objects in a two-dimensional (2-D) area.

In the recent past, several different localization systems have been presented. Systems to localize objects indoor and outdoor were presented in [9]–[11]. These systems are based on RF- and RADAR sensors, which use special modulated RF signals. On many robotic systems the global positioning system (GPS) is implemented to determine their position, as in [12] and [13]. Other systems are based on sonar sensors [14], [15] by which the environment is scanned to define the position. Optical systems were used in [16]–[18] to localize a moving object. Hereby were LASER or video sensors implemented on the objects.

All of these systems have in common that the objects being localized need a power supply. On the contrary, the SAW ID-tag is working completely passive and, therefore, needs no power supply. Furthermore, the SAW ID-tags are tiny and, with a proper housing, robust against environmental influences such as stress, humidity, and magnetic and electric fields.

Manuscript received September 3, 2002; revised December 4, 2002.

The authors are with the Faculty of Engineering and Natural Sciences, Sabancı University, TR-34956 Orhanli-Tuzla, Turkey.

Digital Object Identifier 10.1109/TMTT.2003.810142

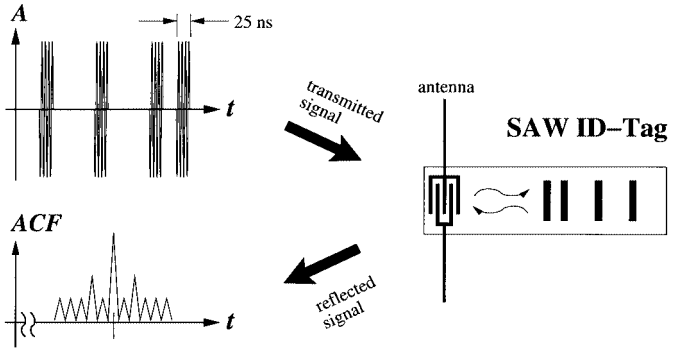

Fig. 1. Identification with means of correlation.

II. Identification

The idea is to identify several objects that are located in an area. Hence, the correlation method for the coded SAW ID-tag is used. Hereby the ID-tag is interrogated with the time inverse of its impulse response [8]. The SAW ID-tag retransmits the correlated signal. If the matched filter condition is fulfilled, the retransmitted RF-signal shows an autocorrelation peak, as depicted in Fig. 1. Only that SAW ID-tag responds with a high amplitude, which is interrogated with its time-inverted impulse response, and meanwhile, the other ID-tags show a far lesser response amplitude.

Therefore, the code of each object within the observed area must be known. For a clear identification, it is necessary to keep the interference low. Special codes are required, which provide a high orthogonality, as shown in [7]. On a computer, all codes of participating objects are stored in a database. The computer sends in each request cycle the time-inverted code sequence of one object. After a delay time, it receives the autocorrelation peak of the targeted object, as well as pseudonoise of the other objects. Fig. 2 shows the measured reflections of one SAW ID-tag provided by Baumer Electric AG, Frauenfeld, Switzerland. The tags used here show the reflected impulses at discrete time positions in a raster of 25 ns. This requires a minimum bandwidth of $B = 40$ MHz to separate two directly adjacent placed impulses. All signals were measured with this bandwidth. However, due to the ID-tag manufacturing process, the position accuracy of each impulse in this raster is better than ± 0.5 ns.

The SAW ID-tag was fed with a 50-Ω source. For this measurement, a simple matching network consisting of one reactive element was used to reduce the insertion loss of the tag. With this matching network, a standing-wave ratio of 2.0 was achieved and the insertion loss of the filter is measured to $\mathrm{IL} = 30$ dB.

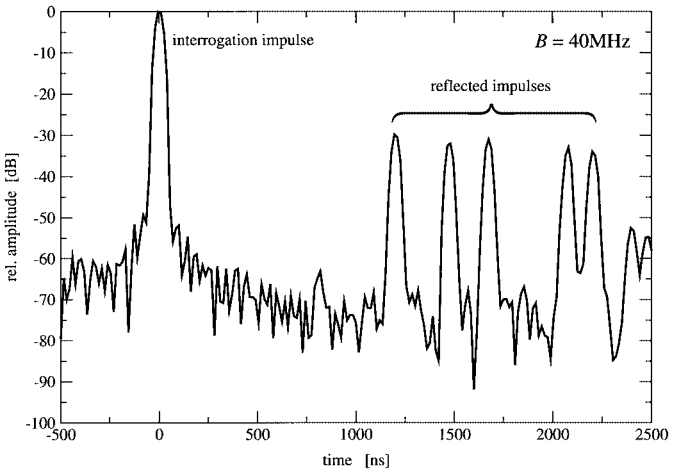

Fig. 2. Measured reflections of an SAW ID-tag.

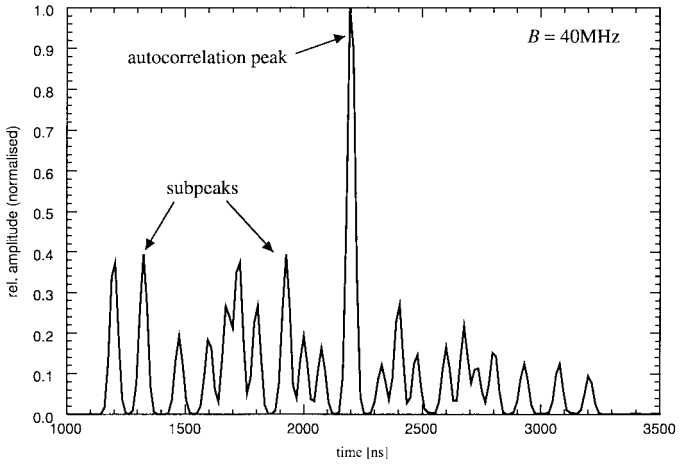

Fig. 3. Autocorrelation signal retransmitted by the SAW ID-tag.

Later on, the antenna for the SAW ID-tag was designed in that way that its impedance made the matching network dispensable.

At the time $t = 0$ s, the interrogation impulse is seen. After the delay time of exactly $t_{\mathrm{delay}} = 1.2\ \mu$s, the reflected impulse sequence starts and lasts $t_{\mathrm{code}} = 1.0\ \mu$s for all SAW ID-tags used here. The reflective delay time of the SAW ID-tag is important for a clear identification and also for the localization. Within this delay time, the environmental echoes of the transmitted signal have ceased and the demodulator, gated during this reflective delay time, evaluates the reflected impulse sequence. With this kind of SAW ID-tag, five peaks at certain time positions in a raster of 25 ns define the coding. The SAW ID-tag is interrogated with the time inverse of its impulse response and retransmits the autocorrelated signal, as shown in Fig. 3. The power amplitude is presented in linear scale and has been normalized.

The impulses of the interrogation signal are generated with an RF switch. Each pulse has a width of 20 ns, whereas the rise and fall times due to the RF switch are $t_{\mathrm{r}} = t_{\mathrm{f}} = 10$ ns. Also here, the bandwidth was $B = 40$ MHz. The correlation process begins after $t_{\mathrm{delay}} = 1.2\ \mu$s and lasts until $2t_{\mathrm{code}} = 2.0\ \mu$s. The time between the entering of the pulse sequence to the SAW chip and the exiting of the reflected autocorrelation peak from the SAW chip is defined here as T_{SAW} and measured to be 2.2 μs.

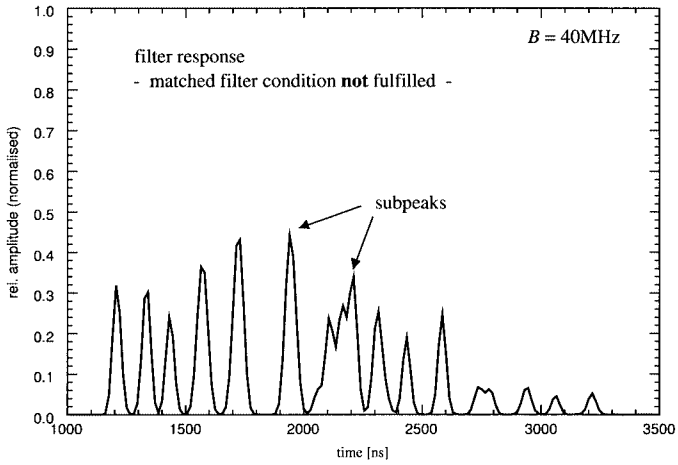

Fig. 4. Cross-correlation signal of another SAW ID-tag.

For comparison, another SAW ID-tag is being interrogated with the same interrogation signal.

Due to a different code, the cross-correlated signal shows only subpeaks with a lower amplitude, as seen in Fig. 4. For the investigation of the multiple access problem later on, the **A**utocorrelation **P**eak amplitude to the **C**ross correlation sub**p**eak amplitude **R**atio is being introduced, which is abbreviated as $APCPR$. With the ID-tags presented here, the $APCPR$ has a value of two.

Both ID-tags show the same insertion loss and were normalized with the same factor. The power of the interrogation signal was also the same for both tags. This means that both ID-tags had the same distance to the transmitter and receiver.

All measurements shown were done at room temperature $T = 20\,^{\circ}$C. The ID-tag was tested in the temperature range from 0 °C to +40 °C, whereas the temperature coefficient of the ID-tag was $\mathrm{TK} = -75$ ppm/K, given by the manufacturer. Within this temperature range, the time shift of the correlation peak was less than 500 ps. The amplitude decreased hereby with less than 1%, and the $APCPR$ was not affected.

III. Localization

A. Principle

For the nonambiguous localization of an object in a specified 2-D area, at least three receiving antennas are necessary. Fig. 5 shows one possible constellation of antennas, whereas the receiving antenna 1 is in the same place as the transmitting antenna. The position of the object is defined by the coordinates (r, φ) with the transmitting antenna as the origin. The locus of constant distance $d_{\mathrm{i}} = r + r_{\mathrm{i}}$ $(\mathrm{i} = 1, 2, 3)$ of one pair of antennas is an ellipse, whereas each antenna lies in one focus of the corresponding ellipse. The point where all three ellipses are intersecting is the position of the requested object.

To calculate each ellipse, the coordinates of each receiving antenna i must be known, whereas the transmitting antenna lies in the origin. Herefore, a calibration of the system has to be

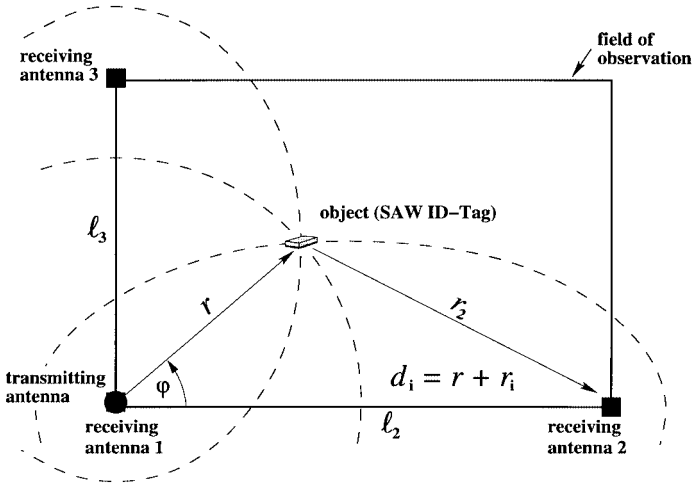

Fig. 5. Localization of an object.

TABLE I
MEASURED TIME DELAYS

System	$T_{\rm sys} = 0.100\mu$s
SAW ID-Tag	$T_{\rm SAW} = 2.200\mu$s
Cable 1 (2m)	$T_{\rm cable,1} = 0.009\mu$s
Cable 2,3 (10m)	$T_{\rm cable,2} = T_{\rm cable,3} = 0.045\mu$s

done: known is the time delay $T_{\rm sys}$, caused by the field-programmable gate array (FPGA), RF switch, and demodulator unit. The time delay $T_{\rm SAW}$ on the SAW ID-tag and the time delay $T_{\rm cable,\,i}$ due to the cables between each receiving antenna and the demodulator is also included in the calibration data. In Table I, the measured time delays are listed, whereas (1)–(3) present the ellipse equations, respectively, the circle equation, in polar coordinates. The signal propagation delay $T_{d,\,\rm i}$ during the distance $d_{\rm i}$ is the total measured time $T_{\rm total,\,i}$ corrected by the calibration data expressed by (4)

$$r = \frac{1}{2}\,d_1 \tag{1}$$

$$r = \frac{\frac{1}{2}\left(d_2^2 - \ell_2^2\right)}{d_2 - \ell_2\cos\varphi} \tag{2}$$

$$r = \frac{\frac{1}{2}\left(d_3^2 - \ell_3^2\right)}{d_3 + \ell_3\cos(\varphi + \pi/2)} \tag{3}$$

$$d_{\rm i} = \frac{T_{\rm total,\,i} - T_{\rm SAW} - T_{\rm sys} - T_{\rm cable,\,i}}{c_0}, \qquad {\rm i} = 1,\,2,\,3. \tag{4}$$

In these equations, the parameters d_1, d_2, and d_3 are indirectly measured, whereas the distances ℓ_2 and ℓ_3 are directly measured, and c_0 is the speed of light in vacuum.

B. Position Accuracy and Cycle Time

The position accuracy is defined by the accuracy of the calibration data and the accuracy of the measured time delay. For an accurate time measurement with sub-nanosecond resolution, a special programmed FPGA is used [19]–[21]. With such a device, the time could be measured within an absolute precision of ± 200 ps at room temperature $T = 20\,^{\circ}$C. This corresponds to a position accuracy of ± 6 cm. For the temperature range from 0 °C to +40 °C, the accuracy decreased to ± 400 ps [21], which corresponds to a position accuracy of ± 12 cm.

The system bandwidth has to be wide enough to detect two adjacent code pulses on the ID-tag. Since the timer module is triggered at the rising edge of the impulse and not by the pulsewidth, the system bandwidth is not limiting the position accuracy as long as this bandwidth is being kept constant over time. As mentioned in Section II, the position accuracy of each code pulse on the SAW ID-tag is better than ± 500 ps, which can be interpreted as the tag bandwidth. This time accuracy results in a position accuracy of ± 15 cm.

Furthermore, the error of the antenna location effects the position accuracy. This error, determined to ± 0.5 cm, is far smaller than the error due to the time measurement and is, therefore, negligible.

In a closed environment, the retransmitted correlation peak causes echoes like the sent interrogation signal. These echoes always go through a longer distance to the receiving antennas than the direct signal. Since the timer module is triggered at the rising edge of the retransmitted signal, the first received impulse is being evaluated. However, when the object is close to a reflective wall, the delay time difference between the echo signal and the direct signal is nearly zero. Direct signal and echo are smearing and the width of the evaluated correlation peak is widening. This causes a reduced time measurement accuracy. Hence, it has to be guaranteed that the delay time difference shows a value of more than approximately 1 ns to avoid this effect. This can be realized, for example, by placing the receiving antennas 30 cm away from each wall.

All objects in an area are interrogated sequentially. The time between the interrogation of the first and last object is called the cycle time $T_{\rm cycle}$. This cycle time depends on the number of objects and the size of the observed area. Dominant hereby is the time delay $T_{\rm SAW} = 2.2\ \mu$s of the SAW ID-tag

$$\begin{aligned} T_{\rm cycle} &\geq n \cdot \left(T_{d,\,\max} + T_{\rm SAW} + T_{\rm sys} + T_{\rm cable,\,max} + T_{\rm comp}\right) \\ &= n \cdot \left(T_{\rm total,\,max} + T_{\rm comp}\right) \end{aligned} \tag{5}$$

where n is the number of objects, $T_{\rm total,\,max}$ is the maximum total signal propagation delay, and $T_{\rm comp}$ is the computation time of the computer to process and store the data. Assuming, for example, ten objects in an area of 30×30 m^2 yields a cycle time of $T_{\rm cycle} \approx 30\ \mu$s.

C. Maximum Detection Range

The maximum detection range is described by the following equation, which is known as the *radar* equation [22], [23]. Since the distance r between the transmitter and the SAW ID-tag and the distance $r_{\rm i}$ between the SAW ID-tag and the receiving antenna are not the same, the *radar* equation is expressed as

$$r \cdot r_{\rm i} = \left(\frac{\lambda}{4\pi}\right)^2 \cdot \sqrt[2]{\frac{P_0 G_{\rm t} G_{\rm r} G_{\rm s}^2}{\rm IL \cdot k T_0 B F \cdot SNR}} \tag{6}$$

where

$r \cdot r_\mathrm{i}$	maximum distance product between transmitter, SAW ID-tag and receiving antenna;
λ	electromagnetic wavelength;
P_0	transmitted power;
G_t G_r	respective gains of the transmitting and receiving antennas;
G_s	gain of the SAW ID-tag antenna;
IL	insertion loss of the SAW device;
kT_0BF	thermal noise power (Boltzmann's constant k, absolute temperature T_0, system bandwidth B, noise figure F);
SNR	required minimum SNR to detect the received signal with a specific rate or probability of errors.

The solution of (6) is a fourth-order curve (*Cassini Oval*), transmitter and receiving antenna at its two foci. The maximum observation area can be fitted into the area of this curve. The SAW ID-tag is designed for the frequency $f = 2.5$ GHz. The insertion loss was measured to $\mathrm{IL} = 30$ dB. The maximum transmitted power P_0 is defined on the one hand by the maximum input power of the SAW ID-tag and on the other hand by the maximum admissible radiation [24]. A value of $P_0 = 1$ W was chosen. The transmitting and receiving antennas used here are patch arrays and have a gain of $G_\mathrm{t} = G_\mathrm{r} \approx 12$ dBi. The ID-tag antenna has a gain of $G_\mathrm{s} \approx 6$ dBi. Due to the active receiving antennas, the noise figure of the receiving system is $F = 3$ dB, whereas the bandwidth of the system is $B = 40$ MHz. An SNR of 10 dB is required to detect the signal. Based on these data and for a single request cycle, the product $r \cdot r_\mathrm{i}$ is approximately 100 m^2. This corresponds to a square observation area of 7×7 m^2, assuming the antenna constellation in Fig. 5.

D. Multiple Access

In the presence of several objects, the correlated and retransmitted signals from the ID-tags overlap in time. This is because the time for the correlation process ($2t_\mathrm{code}$) is much longer than the signal delay time in free space. There is the case when the distance d_i of the requested object $\mathbf{A}$ is greater than the distance of the nonrequested object $\mathbf{B}$. In this case, the in the demodulator received power amplitude of the autocorrelation peak can be lower than the power amplitude of the subpeaks. Hence, the autocorrelation peak cannot be detected. For a given distance product $(r \cdot r_\mathrm{i})_\mathbf{B}$ of the nonrequested object $\mathbf{B}$, the maximum distance product $(r \cdot r_\mathrm{i})_\mathbf{A}$ of the requested object $\mathbf{A}$ can be calculated. Using (6) yields the relation between the distance products with the $APCPR$ as the parameter

$$(r \cdot r_\mathrm{i})_\mathbf{A} = \sqrt{APCPR} \cdot (r \cdot r_\mathrm{i})_\mathbf{B}. \tag{7}$$

For a given position of the requested object $\mathbf{A}$, Fig. 6 shows how close the nonrequested object $\mathbf{B}$ to a transmitting–receiving antenna pair can come so that a detection of the autocorrelation peak is still possible. The requested object $\mathbf{A}$ is situated at the limit value of the observation area of 100 m^2, as shown in Fig. 6. Each $APCPR$ gives the corresponding positions of the nonrequested object $\mathbf{B}$, as denoted by the arrows. Hence, the maximum observation area is reduced by a decreasing $APCPR$.

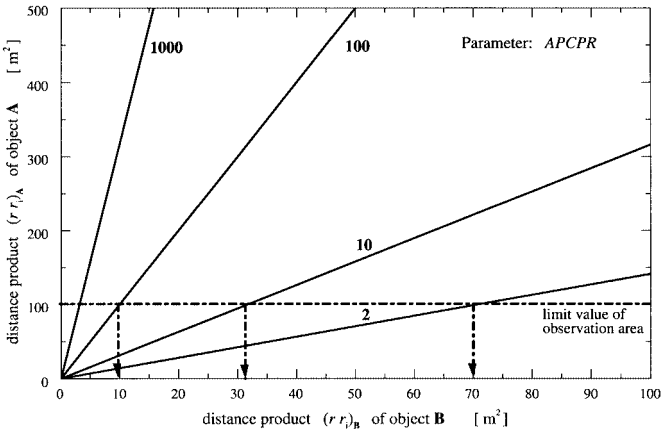

Fig. 6. Maximum distance product relation with the parameter $APCPR$.

TABLE II
MAXIMUM OBSERVATION AREA DEPENDENT ON $APCPR$

$APCPR$	max. observation area
2	0.7×0.7m²
10	2.6×2.6m²
100	4.8×4.8m²
1000	5.7×5.7m²

For some given $APCPR$s, Table II presents the corresponding maximum observation area that was computed numerically.

To keep the maximum observation area as large as possible, the $APCPR$ and, therefore, the code length, must increase. However, long codes are hardly realizable, as the insertion loss of the SAW ID-tags will increase.

Another way to identify and localize objects in an as large as possible observation area is to introduce different delay times t_delay for every ID-tag. This means that the correlated and retransmitted signals from each ID-tag do not overlap in time. According to each object, the gate time for the timer module can be adjusted. The code length (t_code) can be reduced by this adjustment in order to avoid too long delay lines. Equation (8) gives the delay time for each object n

$$t_{\mathrm{delay},\,n} = 1.2\ \mu\mathrm{s} + (n-1) \cdot t_\mathrm{code}. \tag{8}$$

Long delay lines in SAW technology cause large chip sizes and also high insertion losses. The cycle time increases. Therefore, the number of objects is strictly limited. However, objects can be traced within the maximum observation area, whereas the $APCPR$ can be low.

IV. SYSTEM

Fig. 7 schematically shows the whole system. A local oscillator at 2.5 GHz together with the RF switch generates the interrogation signal. The RF switch is controlled by an FPGA and a computer.

The following amplifier increases the transmitting power to obtain a larger observation area. The transmitting and receiving antennas were realized by microstrip-line patch-antenna arrays.

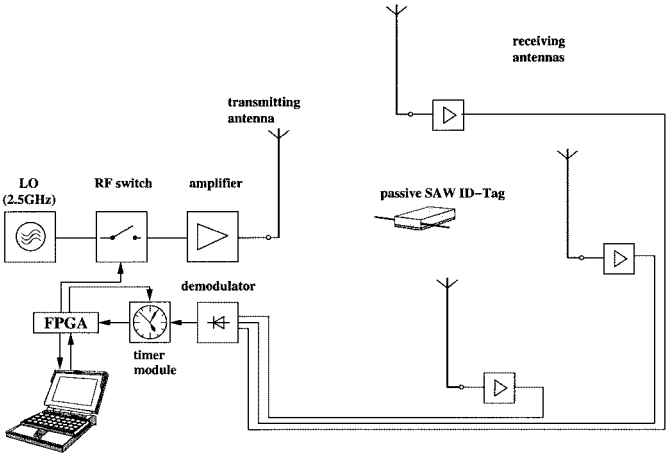

Fig. 7. Identification and localization system.

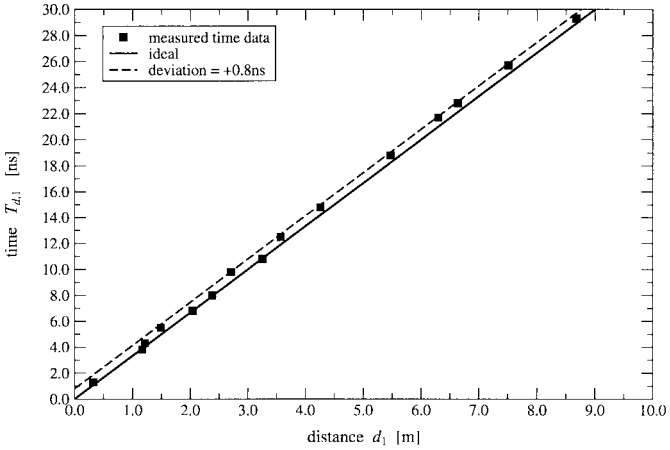

Fig. 8. Measured delay time $T_{d,1}$ versus the distance d_1.

The receiving antennas are active antennas to compensate the negative effects of the long cables between the antennas and demodulator. The negative effects are, on the one hand, the losses and, on the other hand, the capacity of the cable. By the active antennas, the SNR of the receiving system has been increased [25], [26]. Since, for this system, only the magnitude of the received signal is relevant for detection, the demodulator unit is realized with p-i-n diodes. The timer module, realized by special programmed FPGAs [19]–[21], analyzes the received autocorrelation peaks and compares the time delays. Furthermore, the timer module is gated individually for each SAW ID-tag in the time domain during the reflective time delay T_{SAW}. The environmental echoes are below the level of evaluation that makes the system also applicable in rooms. On the computer, the data is being stored and displayed. The path of every identified object can be presented during the observation time.

V. Measurements

A. Accuracy

For tests, an area of 2×2 m^2 has been observed. One SAW ID-tag was placed at arbitrarily chosen positions and the time delays, calibrated with the data given in Table I, have been measured. Fig. 8 shows for antenna 1 the measured delay time $T_{d,1}$ versus the geometrically defined distance d_1. The ideal linear curve ($T_{d,1} = d_1/c_0$) is plotted as well as the maximum deviation of $+0.8$ ns to this ideal curve. The maximum deviation of the measured points from the ideal curve is $+0.8$ and -0.2 ns, which corresponds to a distance error of -24 and $+6$ cm, respectively, when vice versa the time is being measured and the distance is being calculated.

The other measurements for the delay time $T_{d,2}$ and $T_{d,3}$ show the same deviation. Table III shows the target values $x_{\mathrm{i,t}}$ and $y_{\mathrm{i,t}}$ of the tag position and the measured positions $x_{\mathrm{i,m}}$ and $y_{\mathrm{i,m}}$ with its deviation.

The position accuracy of the measured values is determined by the intersection region of the min–max ellipses due to the min–max tolerances of the measured delay time $T_{d,\mathrm{i}}$. In this table, the given tolerances are the worst case values and are slightly greater than those discussed in Section III-B.

TABLE III
Coordinates of the SAW ID-Tag

Position i	target value $x_{\mathrm{i,t}}$	target value $y_{\mathrm{i,t}}$
1	$50.0\mathrm{cm}^{\pm 0.5\mathrm{cm}}$	$50.0\mathrm{cm}^{\pm 0.5\mathrm{cm}}$
2	$150.0\mathrm{cm}^{\pm 0.5\mathrm{cm}}$	$150.0\mathrm{cm}^{\pm 0.5\mathrm{cm}}$
3	$180.0\mathrm{cm}^{\pm 0.5\mathrm{cm}}$	$30.0^{\pm 0.5\mathrm{cm}}$
Position i	**measured value $x_{\mathrm{i,m}}$**	**measured value $y_{\mathrm{i,m}}$**
1	$63\mathrm{cm}^{+14\mathrm{cm}}_{-21\mathrm{cm}}$	$59\mathrm{cm}^{+14\mathrm{cm}}_{-21\mathrm{cm}}$
2	$159\mathrm{cm}^{+14\mathrm{cm}}_{-21\mathrm{cm}}$	$153\mathrm{cm}^{+14\mathrm{cm}}_{-21\mathrm{cm}}$
3	$187\mathrm{cm}^{+14\mathrm{cm}}_{-21\mathrm{cm}}$	$39\mathrm{cm}^{+14\mathrm{cm}}_{-21\mathrm{cm}}$

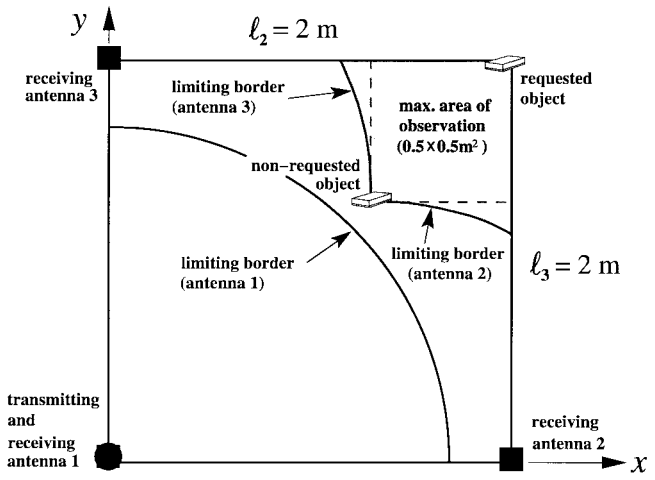

Fig. 9. Maximum observable area for multiple access (two SAW ID-tags).

B. Multiple Access

In another test, two SAW ID-tags with different codes and an $APCPR$ value of two were placed into the observation area of 2×2 m^2. The requested tag was placed at the position $x = y =$

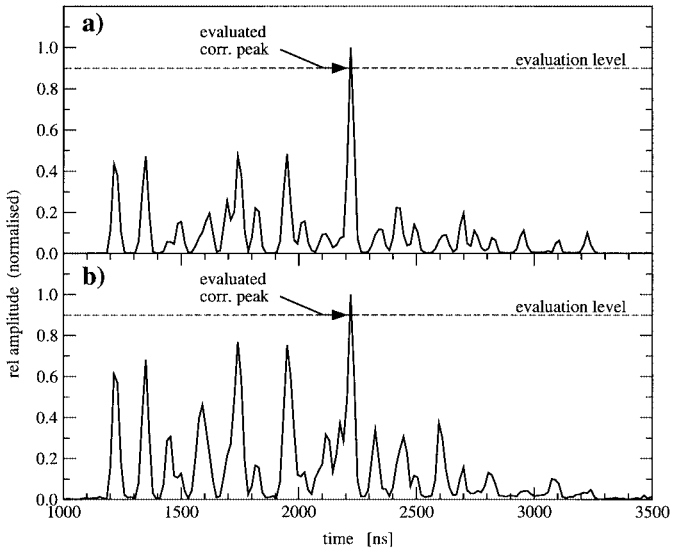

Fig. 10. Received signal of two interrogated SAW ID-tags. (a) At the same position. (b) Nonrequested ID-tag 80 cm closer to antenna 1.

2 m. The position of the nonrequested tag was then changed within the observation area. At the outputs of each demodulator, the correlation peak has been observed and those positions of the nonrequested tag have been noted when the correlation peak was just detectable. This results in limiting borders for each antenna, as depicted in Fig. 9. Fig. 10 shows the received signal at antenna 1 of two interrogated ID-tags. In Fig. 10(a), the two ID-tags were at the same position $x = y = 2$ m, and in Fig. 10(b), only the nonrequested tag was moved toward antenna 1 by approximately 80 cm.

The reduced maximum observation area of approximately 0.5×0.5 m^2 due to the low $APCPR$ value is marked in Fig. 9 and is slightly smaller than expected (Table II).

VI. Conclusion

With means of SAW ID-tags, a new system for identification and localization has been presented. The advantage of this systems is that the SAW ID-tags are small and passive. Hence, the objects do not need to supply the ID-tag with power. The ID-tags used here are operating at 2.5 GHz. Therefore, objects can be observed in an area of approximately 7×7 m^2. However, this area is reduced by a low $APCPR$ of the ID-tags in the case of multiple access. The position accuracy was determined to be approximately ± 20 cm.

The area of observation can be increased by reducing the operating frequency. However, the industrial–scientific–medical (ISM) band is quitted and, therefore, so is the license-free operation. Reducing the operating frequency has two effects. The wavelength is directly proportional to the detection range, as seen in (6), and the insertion loss of the SAW device is also reduced. On the other hand, a reduced frequency results in a reduced time resolution of the code and, therefore, a reduced position accuracy. The SAW chip size also enlarges.

Furthermore, the range of detection can be increased by several request cycles. The signal for one object is then averaged, as shown in [3]. Both the decreasing of the frequency and the averaging of the signal are at the expense of position resolution.

For a further increase of the observation area or the use at more complex area shapes, this system can be considered as a unit cell. Several so-called unit cells are matched together to cover a larger or more complex observation area. The interference between theses unit cells can be kept very low by using suitable antenna patterns.

Acknowledgment

The authors would like to thank D. Zehnder and Dr. R. Peter, both of Ident-Systems, Baumer Electric AG, Frauenfeld, Switzerland, for providing the SAW ID-tags and for helpful discussions.

References

[1] L. Reindl, G. Scholl, T. Ostertag, C. C. W. Ruppel, W.-E. Bulst, and F. Seifert, "SAW devices as wireless passive sensors," in *Proc. IEEE Ultransonics Symp.*, 1996, pp. 363–367.

[2] L. M. Reindl, A. Pohl, G. Scholl, and R. Weigel, "SAW-based radio sensor systems," *IEEE Sensors J.*, vol. 1, pp. 69–78, June 2001.

[3] F. Schmidt, O. Sczesny, L. Reindl, and V. Magori, "Remote sensing of physical parameters by means of passive surface acoustic wave devices (ID tag)," in *Proc. IEEE Ultransonics Symp.*, 1994, pp. 589–592.

[4] L. Reindl and W. Ruile, "Programmable reflectors for SAW-ID-tags," in *Proc. IEEE Ultransonics Symp.*, vol. 1, 1993, pp. 125–130.

[5] L. M. Reindl, G. Scholl, T. Ostertag, W. Ruile, H. Scherr, C. C. W. Ruppel, and F. Schmidt, "Wireless remote identification and sensing with SAW devices," in *Proc. Sensors*, vol. 1, 1997, pp. 161–166.

[6] K. Yamanouchi, G. Shimizu, and K. Morishita, "2.5 GHz SAW propagation and reflection characteristics and application to passive electronic tag and matched filter," in *Proc. IEEE Ultransonics Symp.*, 1993, pp. 1267–1270.

[7] G. Ostermayer, A. Pohl, L. Reindl, and F. Seifert, "Multiple access of SAW sensors using matched filter properties," in *Proc. IEEE Ultransonics Symp.*, Toronto, ON, Canada, 1997, pp. 339–342.

[8] G. Ostermayer, A. Pohl, R. Steindl, and F. Seifert, "SAW sensors and correlative signal processing—A method providing multiple access capability," in *Proc. ISSSTA*, Sun City, South Africa, 1998, pp. 902–906.

[9] M. Lange and J. Detlefsen, "94 GHz 3D-imaging radar for sensor-based locomotion," in *IEEE MTT-S Int. Microwave Symp. Dig.*, vol. 3, 1989, pp. 1091–1094.

[10] C. Dionisio, "Detection and localization of lost objects by SAR technique," in *Int. Geoscience and Remote Sensing Symp.*, vol. 1, 1996, pp. 28–30.

[11] N. Bulusu, J. Heidemann, and D. Estrin, "GPS-less low-cost outdoor localization for very small devices," *IEEE Pers. Commun.*, pp. 28–34, Oct. 2000.

[12] P. Goel, S. I. Roumeliotis, and G. S. Sukhatme, "Robust localization using relative and absolute position estimates," in *IEEE/URSJ Int. Intelligent Robots and Systems Conf.*, vol. 2, 1999, pp. 1134–1140.

[13] S. Panzieri, F. Pascucci, and G. Ulivi, "An outdoor navigation system using GPS and inertial platform," *IEEE/ASME Trans. Mechatron.*, vol. 7, pp. 134–142, June 2002.

[14] L. E. Navarro-Serment, C. J. J. Patedis, and P. K. Khosla, "A beacon system for the localization of distributed robotic teams," in *Proc. Int. Field and Service Robotics Conf.*, Pittsburgh, PA, Aug. 1999.

[15] Z. Feng-ji, G. Hai-jiao, and K. Abe, "A mobile robot localization using ultrasonic sensors in indoor environment," in *IEEE Int. Robot and Human Communication Workshop*, 1997, pp. 52–57.

[16] C. Pegard and El-M. Mouaddib, "A mobile robot using a panoramic view," in *IEEE Int. Robotics and Automation Conf.*, vol. 1, Apr. 1996, pp. 762–777.

[17] L. Delahoche, El-M. Mouaddib, C. Pegard, and P. Vasseur, "A mobile robot localization based on a multisensor cooperation approach," in *IEEE Int. Industrial Electronics, Control, and Instrumentation Conf.*, vol. 1, 1996, pp. 155–160.

[18] S. Panzieri, F. Pascucci, R. Setola, and G. Ulivi, "A low cost vision based localization system for mobile robots," in *9th Mediterranean Control and Automation Conf.*, Dubrovnik, Croatia, June 2001.

[19] E. Räisänen-Ruotsalainen, T. Rahkonen, and J. Kostamovaara, "An integrated time measurement unit with 10μs measurement range and subnanosecond resolution," in *Proc. NORCHIP '92 Seminar*, Helsinki, Finland, Nov. 1992, pp. 99–105.
[20] ——, "An integrated time-to-digital converter with 30-ps single-shot precision," *IEEE J. Solid-State Circuits*, vol. 35, pp. 1507–1510, Oct. 2000.
[21] R. Szplet, J. Kalisz, and R. Szymanowski, "Interpolating time counter with 100 ps resolution on a single FPGA device," *IEEE Trans. Instrum. Meas.*, vol. 49, pp. 879–883, Aug. 2000.
[22] M. I. Skolnik, *Introduction to Radar Systems*. New York: McGraw-Hill, 1979.
[23] C. E. Cook and M. Bernfeld, *Radar Signals*. Norwood, MA: Artech House, 1993.
[24] Int. Commission Non-Ionizing Rad. Protection, "Guidelines for limiting exposure in time-varying electric, magnetic and electromagnetic fields (up to 300 GHz)," *Health Phys.*, vol. 74, no. 4, pp. 494–522, Apr. 1998.
[25] H. H. Meinke and F. M. Landstorfer, "Noise and bandwidth limitations with transistorized antennas," in *IEEE Int. Antennas and Propagation Conf.*, Boston, MA, Sept. 1968, pp. 245–246.
[26] H. Lindenmeier, "Transistorized receiving antennas," in *Int. URSI Electromagnetic Waves Symp.*, 423 A, Munich, Germany, 1980.

Thomas F. Bechteler was born in Munich, Germany, in 1968. He received the Dipl.-Ing. degree from the Technical University of Munich, Munich, Germany, in 1997, and the Dr.-Ing. degree from the University of the Armed Forces, Munich, Germany, in 2001.

From 1996 to 1997, he was with the German Aerospace Center DLR. He is currently a Post-Doctoral Research Fellow with the Faculty of Engineering and Natural Sciences, Sabancı University, Orhanli-Tuzla, Turkey. He is engaged in research and development of RF/microwave devices and circuits.

Hüsnü Yenigün was born in Turkey. He received the B.Sc. and Ph.D. degrees in electrical and electronics engineering from the Middle East Technical University (METU), Ankara, Turkey, in 1992 and 2000, respectively.

From 1992 to 1997, he was with the Scientific and Technical Research Council of Turkey (TÜBİTAK). From 1997 to 2000, he was with Bell Laboratories. He is currently with the Faculty of Engineering and Natural Sciences, Sabancı University, Orhanli-Tuzla, Turkey. His areas of interest are formal methods, hardware/software verification, and model checking in computer science.